Mechanical Signals Trigger Myosin II Redistribution and Mesoderm Invagination in *Drosophila* Embryos

Philippe-Alexandre Pouille°, Padra Ahmadi°, Anne-Christine Brunet and Emmanuel Farge*
UMR 168, CNRS, Institut Curie
11 rue Pierre et Marie Curie, 75005 Paris

*Corresponding Author : efarge@curie.fr

° These two authors contributed equally the work

Abstract

During *Drosophila* gastrulation, two waves of constriction occur in the apical ventral cells, leading to mesoderm invagination. The first constriction wave is a stochastic process that is mediated by the constriction of 40% of randomly positioned mesodermal cells and is controlled by the transcription factor Snail. The second constriction wave immediately follows and involves the other 60% of the mesodermal cells. The second wave is controlled by the transcription factor Twist and requires the secreted protein Fog. Complete mesoderm invagination requires redistribution of the motor protein Myosin II to the apical side of the constricting cells. We show that apical redistribution of Myosin II and mesoderm invagination, both of which are impaired in *snail* homozygous mutants that are defective in both constriction waves, are rescued by local mechanical deformation of the mesoderm with a micromanipulated needle. Mechanical deformation appears to promote Fog-dependent signaling by inhibiting Fog endocytosis. We propose that the mechanical tissue deformation

that occurs during the Snail-dependent stochastic phase is necessary for the Fog-dependent signaling that mediate the second collective constriction wave.

INTRODUCTION

Embryos develop through the biochemical processes that control the patterning and geometrical morphogenesis of multicellular tissues [1-4]. Animal morphogenesis initiates at gastrulation, a process of genetically controlled active shape changes of the tissue that lead to the formation of the ectoderm, endoderm, and mesoderm layers. In *Drosophila* embryos, gastrulation begins with mesoderm invagination, which is followed by germ-band extension, and both of these processes are morphogenetic movements that are regulated by polarized distribution of Myosin II (MyoII, encoded by the *zipper* gene) within the submembrane cortex of the motor cells generating the movements [5-7]. The mechanical strains associated with morphogenesis also serve as signals that feedback into biochemical processes that regulate patterning and into the gene expression profiles that regulate development [8-11]. Here, we report that the mechanical events that occur at the earliest stages of gastrulation also provide a signal that feeds into the posttranslational events actively controlling morphogenesis. The mechanical cues trigger the concentration of MyoII at the apical side of the cells, which constricts the cells to produce mesoderm invagination.

The genetic network that controls the *Drosophila* embryo mesoderm invagination is activated by the maternally supplied transcription factor Dorsal, which translocates to the nucleus to initiate the invagination process. Dorsal stimulates the expression of the genes *Twist* (*Twi*) and *Snail* (*Sna*), which encode transcription factors, in the mesodermal cells [2]. Both factors

are involved in the genetic control of the cell shape changes necessary for the two constriction waves that lead to mesoderm invagination [12-15]. Flies with mutations in *twi* are defective in the second constriction wave, due to deficiency of a secreted signal protein Fog, which is necessary for stable redistribution of the molecular motor MyoII to the apical side of the cells that triggers the coordinated collective constriction [5, 15-17]. Flies with mutations in *sna*, which still express *fog* [18], are defective in both the first stochastic waves and in the second collective wave. Thus, Snail and Fog are together necessary for the second collective constriction wave [19]. Here, we report the existence of a mechanical cue that controls Fog signaling, Myo-II redistribution, and constriction of the cells along the apical surface of the embryo, which provides a mechanistic scenario for the interplay between Snail and Fog in controlling mesoderm invagination. The Snail-dependent stochastic phase produces a mechanical signal that feeds into the Twist-dependent collective constriction phase.

RESULTS

Mechanical rescue of mesoderm invagination and apical redistribution of MyoII in *sna* embryos

To test the hypothesis that a mechanical cue triggers MyoII redistribution, the *sna* homozygous mutant embryos, which lack the mechanical strain associated with the lack of the 4-min stochastic constriction phase [13], were subjected to a local 3 to 7 μm deformation with a micromanipulated needle. This 4-min indentation was applied to the mesoderm precisely 2 to 3 min after the end of ventral cellularization, the stage at which the first constriction wave would occur in wild-type embryos (Fig. 1A and Fig. S1). Local mechanical indentation rescued a complete mesodermal invagination in 67% of the embryos (Fig. 1B, C, Fig. 2). No

mesoderm invagination was observed in nonindented *sna* homozygous embryos, and ventral flattening was only observed in 25% of cases (Fig. 1C, Fig. S2). The invagination initiated 2 to 3 minutes after indentation, and propagated all along the mesoderm.

The distribution of MyoII in wild-type, *sna*-/*sna*- and indented *sna*-/*sna*- embryos was investigated by immunolabeling (Fig. 2) and is summarized in Fig. 1C. Embryos were considered positive for apical redistribution of MyoII if the protein concentrated at the apical membrane cortex of the mesodermal cells leading to a thin concentration of signal at the membrane [5]. Like in the mesodermal cells of the wild type (Fig. 2), MyoII became concentrated in the apical portion of the cells in 93% of indented *sna*-/*sna*- embryos (Fig. 2). No apical redistribution of MyoII was observed in 75% of the unperturbed *sna* embryos (Fig. 2) (with the remaining 25% exhibiting only a slight redistribution of MyoII and ventral flattening, Fig. S2).

When the mesoderm was locally indented 10 minutes after the end of ventral cellularization (equivalent to the mid-mesoderm invagination stage for a wild type), the indented embryo showed a partial or small active invagination in 62% of the embryos, and a complete invagination in 38% of cases, with apical redistribution of MyoII occurring only in the invagination domains in all cases (Fig. 2) . When the mesoderm was touched by the needle without deformation, neither mesoderm invagination nor apical redistribution of MyoII was observed, showing that mechanical deformation of mesoderm tissues is required to rescue the *sna*- phenotype (Fig. S3) . Thus, a mechanical cue rescues apical MyoII redistribution and mesoderm invagination in *sna* mutant embryos, with the most efficient rescue occurring when the mechanical indentation is applied to the mesodermal cells at stages equivalent to the Snail-dependent endogenous deformation in the wild type.

As MyoII apical relocation was observed in the mesoderm only, we investigated whether this feature was specific to exogenous indentation of the mesoderm or if global deformation of the tissue could trigger apical redistribution of MyoII outside of the mesoderm in *sna* mutants. Applying a 4 min long global uni-axial deformation to the *sna* mutant embryo[10] at the beginning of stage 6, which increases the embryo's dorsoventral size 10% to 20%, led to MyoII apical redistribution in mesodermal cells only, and to the rescue of a thin and unclosed invagination in 64% of the embryos (Fig. 1C, Fig. 2).

Fog in the mechanical rescue of apical redistribution of MyoII in *sna* embryos

Because the mechanical activation of MyoII redistribution that drives the invagination of *sna* mutants is restricted to the mesoderm cells, we investigated whether the presence of Twist was necessary for the mechanical rescue of *sna* mutant invagination. After indentation of *sna twi* double mutants, neither apical MyoII redistribution (Fig. 3A) nor mesoderm invagination was rescued (Fig. 1C), showing the necessity of the Twist pathway for MyoII redistribution.

Because Fog is downstream of Twist and necessary for MyoII apical redistribution [5, 14], we investigated whether Fog was required for MyoII apical redistribution in response to mechanical cues. We mechanically manipulated *twi sna / twi;PE-Fog* embryos, in which *Fog* expression, altered by *twi* mutations, is rescued under the control of the proximal element of the *twi* promoter (PE) in the mesoderm only [19]. The expression of *snail* is strongly reduced in *twist* mutants at stage 5 [20], thus we anticipated that the expression of *snail* in these embryos lacking both copies of *twi* and one copy of *sna* would be reduced enough to provide a background phenotype equivalent to a *sna twi* mutant at stage 6. Indeed, all Twist-labelled embryos deficient in Twist did not invaginate and showed no anterior midgut invagination

from stage 6 to stage 8, like the *sna twi* mutants showed (Fig. S4A). The Myo-labelled furrow formation-defective embryos lack any apical MyoII redistribution (Fig. 1C and Fig. 3B). Thus, forced expression of Fog in the mesoderm of embryos deficient in Twist and Snail fails to rescue invagination and MyoII apical redistribution in the mesoderm. In contrast, local deformation of these embryos in the mesoderm rescued ventral furrow formation and apical MyoII redistribution in all cases (Fig. 1C, Fig. 3B, and Fig. S4B). No such rescue was observed in the absence of forced expression of Fog in *twi sna / twi* indented embryos (Fig. 1C, Fig. S5). Because *twi sna / twi;PE-Fog* embryos express *Fog*, but do not express other targets downstream of *twi*, the Fog signaling pathway is the relevant target involved in the mechanotransduction pathway that stimulates MyoII apical redistribution. Therefore, both mechanical strain and Fog are necessary and sufficient for the rescue of apical MyoII redistribution and mesoderm invagination in *sna*-deficient embryos.

Endocytosis in mesoderm invagination and apical redistribution of MyoII

Because Fog is required for mechanical cues to trigger MyoII apical redistribution, we investigated the underlying mechanism that translates the mechanical strain signal into activation of the Fog signaling pathway. Fog is an apically secreted protein that most likely signals by binding to a receptor [5, 14]. It is also expected that the Fog-receptor complex may be regulated by endocytosis and receptor recycling or ligand and receptor lysosomal degradation. The initiation of mesoderm invagination correlates with external blebs of apical membranes [16], consistent with an increase of mesoderm cell internal pressure associated with apical flattening and cell shape changes associated with constriction [21]. These processes alter membrane tension and increase outward membrane curvature, which could block endocytosis

and thereby enhance the Fog signaling pathway by blocking the endocytosis of the putative Fog-receptor complex [22, 23]. *shibire* is a temperature-sensitive conditional mutant of dynamin and shifting flies with this mutation to 28°C rapidly and reversibly blocks endocytosis. Thus, we constructed a *shi sna* double mutant line to mimic the putative mechanical inhibition of endocytosis in mesodermal cells that would be lacking in the *sna* embryos because they lack the first constriction wave. After the *shi sna* embryos were laid at 20°C, they were shifted to 30°C for 5 minutes and then returned to 20°C for 15 minutes and then fixed. Double mutants homozygous embryos fixed at late stage 6 and stage 7 exhibited a rescue of both the MyoII apical redistribution and the invagination of the mesoderm (n=7), compared to homozygous embryos developing at 20°C in which only small fluctuations in mesoderm curvature initiated (Fig. 1C and Fig. 4A). No such rescue was observed in heat-shocked *sna* homozygous embryos (Fig. 1C and Fig. S6A). Thus, blocking endocytosis rescues MyoII apical redistribution and mesoderm invagination in *sna*-defective mutants, suggesting that this may be a mechanism by which mechanical cues control the second wave of cell constriction that mediates mesoderm invagination.

The intracellular distribution of Fog at stage 5 and stage 6 is consistent with a block in Fog endocytosis occurring as the mechanical signal is generated in response to the first stochastic cell constriction. Whereas at stage 5, Fog was diffusely localized throughout the cytoplasm of mesoderm cells with little apical concentration in all 12 embryos observed, by mid-stage 6 embryos having initiated apical flattening and constriction showed an apical redistribution of cytoplasmic Fog towards the membrane and Fog was visible at the apical cell surface which is directly adjacent to cytoplasmic concentration just beneath the plasma membrane, in all 11 embryos observed (Fig. 4B). In contrast, the Fog distribution of mid-stage 6 *sna* homozygous mutants embryos, which do not flatten and do not constrict, remained concentrated diffusely

localized throughout the cytoplasm, with poor redistribution towards the apical side of the cell and no Fog at the cell surface in all 10 embryos observed (Fig 4C). Both the retention of secreted signaling proteins at the cell surface and the intracellular accumulation of secreted vesicles are consistent with a mechanical strain on the plasma membrane blocking endocytosis [22, 23] and driving exocytosis [24], leading to an increase of the association of Fog with the cell surface, presumably bound to its receptor, in early stage 6 wild-type embryos, but not in early stage 6 *sna* mutant embryos that are defective in mechanical deformations associated with apical flattening and cell constriction.

To confirm that a block in endocytosis altered Fog distribution in mesoderm cells, we analyzed Fog distribution following heat shock in the *sna shi* mutants. We found Fog accumulated on the apical side of the cells in all 10 embryos examined (Fig 4D) and accumulated on the cell surface of apically flattened cells in 70% of the embryos examined after a 5-minute incubation at 30°C at mid-stage 6 (Fig 4D). In contrast, *sna shi* embryos that were not subjected to heat shock failed to exhibit redistribution of Fog in all 7 embryos examined (Fig. 4D). Even though some cytoplasmic apical increase of concentration was observed, possibly due an increase in endocytosis and exocytosis activity at 30°C, no massive apical attraction of Fog, and no plasma membrane accumulation was observed in all of 10 heat-shocked *sna* homozygous embryos at stage 6. (Fig. S6B). The *shi* mutation blocks endocytosis at 28°C, thus plasma membrane retention of Fog likely reflects a block in Fog endocytosis in *sna shi* stage 6 mutants at 28°C. Note that accumulation of Fog at the apical side of the cells is also observed, which is consistent with an enhancement of exocytosis due to the increase in membrane tension triggered by the apical flattening and contraction of the cells after activation of Fog signaling.

To check whether mechanical cues could block of Fog endocytosis, we monitored Fog distribution in stage 6 *sna* homozygous mutant embryos that were subjected to local indentation. Local indentation triggered the accumulation of Fog on the apical side of the cells in all 6 embryos observed (Fig. 4C), with Fog accumulating at the cell surface in 4 of the 6 embryos (Fig. 4C). This shows a mechanical rescue of the inhibition of Fog endocytosis by indentation in mid-stage 6 *sna* mutant embryos that are defective in stochastic constriction and the associated mechanical deformation.

The proposal that mechanical inhibition of Fog endocytosis is the primary mechanotransduction mechanism activating signaling downstream of Fog and leading to the apical redistribution of MyoII to in response to Snail-dependent stochastic constrictions is supported by three lines of evidence: (i) a Fog-dependent mechanotransduction pathway regulates MyoII apical redistribution (Fig. 3), (ii) blocking endocytosis phenocopies the mechanical rescue of MyoII apical redistribution and mesoderm invagination of *sna* mutants (Fig. 4D), and (iii) the apical membrane accumulation of Fog that is observed in stage 6 wild types (Fig. 4A) is mechanically rescued in *sna* stage 6 mutants by indentation (Fig. 4C),

We, thus, propose that the first stochastic constriction of 40% of mesodermal cells inhibits Fog endocytosis in the other 60% of cells, due to the increase in apical membrane tension induced by apical surface stretching or an increase in cell pressure, and the enhanced Fog signaling then triggers the redistribution of MyoII in these cells.

Simulating the interaction between Fog and Snail in Myo-II apical redistribution

Interestingly, ectopic expression of Fog leads to ectopic MyoII apical redistribution [5], and to apical constriction [18], in domains other than the mesodermal domain defined by the presence

of Snail. Thus, in apparent contradiction with the necessity for Snail and Fog to generate apical constriction, Fog without Snail can also trigger apical constriction. The explanation for how both Fog and of Snail are necessary for MyoII apical redistribution and collective apical contraction in mesoderm cells, but not in nonmesodermal cells in which Fog alone is sufficient, remained a missing link in understanding the control of the early *Drosophila* embryo mesoderm invagination. Because mechanical strains propagate rapidly over long distances, Snail and Fog could be necessary for MyoII apical redistribution without being present in the same cells. Indeed, in embryos ectopically expressing Fog outside of the mesoderm, Snail-initiated stochastic deformations of the mesoderm, which normally lead to the wild type mesoderm collective constriction, could be transmitted mechanically into regions of the embryo where Snail is not present but where Fog is overexpressed [5]. We tested the plausibility of this scenario *in silico* by predicting the phenotype of embryos constitutively overexpressing Fog with a previously developed simulation of the multicellular invaginating embryo [21] to which we incorporated a Snail-dependent stochastic apical constriction process, a mechanosensitive activation of the Fog signaling pathway, and the presence of Fog in all of the modeled cells. The simulation predicted several previously reported phenotypes that have been reported in vivo [5, 18].

In contrast to finite element simulations in sea urchin embryo[25], which introduce a direct mechanical activation of a change in cell shape initiated by the shape change of the central cell of the invaginating domain, we introduced a stochastic concentration parameter "Csna" (to monitor Snail-dependent stochastic constriction of cells), a concentration parameter "Cfog" (to monitor Fog-dependent apical tension from actin-myosin that was above a membrane tension threshold), and an "Endo" parameter (to monitor the value of the membrane tension threshold, which is dependent on the apical surface tension). The values of

the three parameters were defined for mesoderm cells only in order to mimic a transition from stochastic constriction to collective constriction in the wild-type embryo, before introducing the Cfog and Endo parameters into the Fog+ simulation. Mesoderm stochastic apical flattening and constriction was observed at early stage 6 (Fig. 5A), followed by collective apical flattening and constriction that initiated in all mesodermal cells, which was followed by apical flattening in all nonventral cells. The simulation that included Fog in all of the cells, not just the mesoderm, predicted incomplete invagination at stage 6 due to Fog-dependent mechanical activation of lateral and dorsal apical constriction tension, whereas the simulation with Fog only present in the mesoderm reproduced the wild-type phenotype (Fig. 5A). The model predicts a mechanical activation of MyoII apical redistribution that initiates in mesodermal cells, then occurs in lateral and dorsal cells all around the embryo [5]. The model also predicts apical flattening in *sna* embryos that are expressing Fog ectopically all around the embryo [18] (Fig. S7).

DISCUSSION

Mechanical shape and strains play an important role in the maintenance and the development of organ morphology [26, 27]. Embryogenesis is finely controlled by reciprocal mechanical and transcriptional cues that link developmental gene expression and tissue morphogenesis [8, 9, 16]. Here, we suggest the existence of a posttranslational interplay of active morphogenetic movements with regulation of signaling and protein localization involved in morphogenesis. The mechanical deformations of a given stage of development activate the molecular processes that generate the active forces that control the morphogenetic movements of the next stage. We show that the apical redistribution of Myosin is mechanosensitive through a process that is dependent on a Fog signaling mechanotransduction pathway. We find that mechanical cues block Fog endocytosis at the apical membranes of mesoderm cells in

response to Snail-dependent apical flattening and constriction, either due to direct membrane stretching or to an increase in cell volume pressure. The block in Fog endocytosis likely activates the Fog signaling pathway leading to MyoII apical in all mesoderm cells. In this model, forced Fog expression would be countered by endocytosis-mediated degradation and would not be strong enough to activate the Fog signaling pathway, as indicated by the lack of MyoII apical redistribution and mesoderm invagination in embryos defective in both *twi* and *sna* but that have Fog present in the mesoderm (Fig. 3B). Thus, the presence of Fog without the mechanical strain that blocks its endocytosis is not sufficient to activate MyoII apical redistribution and mesoderm invagination. Experiments with stronger overexpression of Fog might eventually compensate degradation and activate the pathway.

In this mechanotransduction process, the sensor would not be a protein that changes conformation in response to the strain (such as a transmembrane pore [28] or a protein linked to the cytoplasmic cytoskeleton [29]), but rather the sensor would be the membrane itself [22], whose strain state modulates the efficiency of the endocytosis of Fog signaling molecules, thereby enhancing the downstream signaling pathway. The modulation of T48 endocytosis, the other protein that is downstream of Twist and is known to participate to mesoderm invagination in parallel of Fog [20, 30], might additionally enhance MyoII apical redistribution, even though Fog only is required in the mechanotransduction processs (Fig. 3). We thus propose a model in which the Fog-dependent mechanical activation of the apical redistribution of MyoII is used to produce a collective apical constriction leading to an efficient invagination in response to the stochastic contraction of Snail-containing cells (Fig. 5B).

Interestingly, response to stress appears to also be involved during plant early morphogenesis, during which microtubules orientate along the mathematically predictable stress field lines of

the developing meristem [31], with this orientation following a potentially active [32] or passive (subcellular minimization of elastic energy) process.

Standard views of embryonic development focus on the control of patterning and of morphogenesis by the genome [33], with demonstrations of a reversal interaction from morphogenesis to the expression status of the genome [9, 10]. The existence of such a bidirectional interplay between the genome and the macroscopic morphology of the embryo shows that some vital aspects of embryogenesis belong to emerging properties of a reciprocal coupling between the morphology and the genome [8]. However, amongst the schemes of interplays controlling embryonic development including these new concepts (gene-to-gene – patterning, gene-to-shape –morphogenesis, and shape-to-gene – mechanical induction of gene expression), evidence for the shape-to-shape interplay (mechanical activation of biochemical pathways triggering active morphogenetic movements of embryogenesis) has been lacking. Here, we describe such a link, through the Fog-dependent mechanical activation of collective and synchronized constriction in response to the Snail-dependent stochastic constriction of mesoderm cell apexes, which allows mesoderm invagination.

We speculate that the use of mechanical activation of MyoII apical redistribution during mesoderm invagination might have evolved from an active invagination feeding reflex of early embryos, putatively dependent on external mechanical strains interrupting the endocytic flow of a secreted protein like Fog [34, 35]. Such a scenario, already suggested at the origin of the mechanical induction of *twi* during early gastrulation [10], would involve a more rapid response through posttranscriptional rather than transcriptional mechanisms.

EXPERIMENTAL PROCEDURES

Strains and labelling

Wild types were Oregon R, Sna^{IIG}/Cyo *sna* mutants and Shi^{1} *shi* mutant were from Bloomington, and sna^{IIG} twi^{IIH}/SM1 *sna twi* double mutants and twi^{EY53};PE-Fog/SM1 were a generous gift of Maria Leptin. The *sna*shi* cross was realized through classical procedures, and took advantage of the "sleeping" phenotype of *shi* mutants at 28°C to identify the presence of the mutation at any step of the cross. Labelling procedures were classical, with rabbit antibodies against MyoII [36], rabbit antibodies against Twist [37], and rabbit antibodies against Fog [5] generously provided by Roger Karess, Siegfried Roth, and Eric Wieschaus, respectively. The Alexa488 secondary antibody against rabbit IgG was from Molecular Probes. Labelling methods with formaldehyde fixation were classical showing labelling of the complete cell [38], and differ from those in reference [5] in that a heat-methanol fixation method used to specifically preserve protein labelling at plasma membrane [39].

Kymographs, determination of phenotypes and mechanical perturbations

Two complementary methods were used to define the phenotype of the *sna* homozygous embryos. The first one consists of tracing the kymographs of the mesoderm movements during the first 10 minutes of stage 6, which shows a contraction wave associated with apical constriction in the wild type or in the heterozygous (Fig. S1A), whereas the homozygous that does not constrict does not show any contraction wave (Fig. S1A). The second one is the timing of the invagination of the cells in the anterior midgut (AMG), which is delayed in *snail* homozygous compared to the timing in the heterozygous and wild-type embryos (Fig. S1B). The same methods were used to define *twi sna* homozygous phenotypes. The absence of Twist in the indented invaginating embryos was checked by immunolabelling of Twist (Fig. S4). Note that it was not possible to similarly check for the absence of Snail in *sna* embryos due to the poor quality of the currently available antibody against *Drosophila* Snail.

Kymographs were captured with Image J and needle indentation was performed with a Nashigire classical micropipette micromanipulator.

Fig. 1. Mechanical rescue of mesoderm invagination in *sna* mutant embryos.

(**A)** Indentation of homozygous *sna*$^{-}$ embryos. The top shows the arrangement of the single-cell layer with the nuclei of the cells at the apical side of the embryo. The black circles represent cell nuclei. (**B)** Mesodermal furrow invagination at stage 7 (black arrow), reflecting mesoderm invagination, occurs in response to mechanical indentation of 67% of *sna-* embryos (n=15) . Embryos are observed in phase contrast. (**C**) Penetrance of the rescue of mesodermal invagination (denoted I) and MyoII redistribution (denoted M) by mechanical disruption. Ventral flattening was the only evidence of partial mesoderm invagination noted in 25% of cases for the *sna-/sna-* embryos in the absence of mechanical deformation and these embryos only exhibited slight redistribution of MyoII (n=8). Number of cases tested in other configurations are *sna-/sna-* indented 2 to 3 min after cellularization (n=15), *sna-/sna-* indented 10 min after cellularization (n=13), *sna-/sna-* global deformation at stage 6 (n=14), *sna-/sna-* touched embryos (n=3), *sna-/sna-* heat shocked embryos (n=10), *twi-sna-/twi-sna-* indented (n=8), *twi-sna-/twi-sna-* controls (n=5), *twi-sna-/twi-* indented (n=3), *twi-sna-/twi-* controls (n=5), *twi-sna-/twi-;PE-Fog* controls (n=16), *twi-sna-/twi-;PE-Fog* indented (n=12), *sna-shi-/sna-shi-* 20°C (n=4), *sna-shi-/sna-shi-* 30°C (n=7).

Fig. 2. Mechanical rescue of apical redistribution of MyoII in *sna* mutant embryos.

Apical redistribution of MyoII and mesoderm invagination is evident at stage 6 in wild-type (WT) embryos. These phenomenon are not observed in *sna-/sna-* embryos. Local ventral indentation fully restores apical redistribution of MyoII and mesoderm invagination in *sna-/sna-* embryos. When embryos were indented 2 to 3 minutes after cellularization (n = 15),

67% show this full invagination rescue phenotype, with 26% of the embryos showing a partial or small invagination response and 7% not responding, and with 93% showing apical redistribution of MyoII (red arrows). When embryos were indented 10 minutes after cellularization (n = 13) 38% show this full invagination rescue phenotype, with a partial or small active invagination in 62% of the embryos, and with 100% showing apical redistribution of MyoII (red arrows). Global deformation by lateral uni-axial compression restores MyoII apical redistribution and unclosed invagination (red arrows) (n = 14; 64% show this phenotype). Anterior invagination delay (yellow arrows) and lack of mesoderm sagittal compression at stage 6 are phenotypes used to select *sna* homozygotes (see Experimental Procedures section, Fig. S1). To capture mesoderm cells, embryos were imaged at the most ventral cells exhibiting invagination or at most ventral cells in embryos that failed to invaginate. The fluctuations in the cytoplasmic apical intensity of MyoII on the dorsal side of the embryo, which varies as function of small variations in the orientation of the embryo, are due to variations in the depth of the focal plane imaged to find the apical border of the invaginating or noninvaginating most ventral cells. The white stars denote the position of the local indent. Positions 1 and 2 show the propagation of MyoII redistribution and mesoderm invagination all along the mesoderm from the point of indent.

Fig. 3. The Fog signaling pathway is necessary for mechanical induction of apical redistribution of MyoII. (A) Apical redistribution of Myo-II is not rescued in *twi- sna-* homozygous embryos indented ventrally, with only MyoII remaining junctional and cytoplasmic, which is characteristic of stage 7 nonmesodermal cells [17]. Left side is control embryos that were not indented (n=5, all embryos). Right side shows embryos indented 2 to 3 minutes after cellularization. Indented embryos failed to invaginate (n=8, all embryos). **(B)**

Left side is *twi sna/twi;PE-Fog* control embryos that were noninvaginating (n=16, all embryos). Right side shows that local ventral indentation rescues mesoderm invagination and MyoII apical redistribution in *twi sna/twi;PE-Fog* embryos all along the mesoderm (n=12, all embryos) (red arrows). Anterior invagination delay (yellow arrows) and lack of mesoderm sagittal compression at stage 6 (not shown) are phenotypes used to select *sna twi* homozygous, and *sna twi/twi PE-Fog* non invaginating phenotypes (see Experimental Procedures section). The white star denotes the position of the indent.

Fig. 4: Fog and MyoII show apical accumulation of mesoderm cells in response to mechanical inhibition of endocytosis in early stage 6.

(A) Blocking endocytosis of with a temperature-sensitive dynamin mutant (*shi*) rescues apical redistribution of MyoII and mesoderm invagination of *sna shi* mutants (n=7, all embryos) (red arrows). The left image shows a *sna shi* double mutant in which endocytosis was not blocked (n=4, all embryos). In the right side, endocytosis was blocked by transient heat shock. (**B**) Wild-type embryos at stage 5 show little apical cytoplasmic accumulation of Fog in mesoderm cells (red arrows). By mid-stage 6, Fog appears at the plasma membrane (red arrows) and accumulates on the apical side of the cell. (**C**) Mid-stage 6 *sna* embryos lack apical plasma membrane accumulation of Fog (red arrows) and Fog fails to redistribute at the apical membrane. Local indentation (red asterisk) at early stage 6 restores Fog accumulation at the plasma membrane of the mesoderm (red arrows) and apical redistribution. Indented *sna* embryos were imaged from stage 6 to stage 7. (**D**) Heat-shocked *sna shi* embryos at stage 6 (right side) show plasma membrane accumulation of Fog (red arrows) and accumulation of cytoplasmic Fog at the apical side of the mesoderm, in contrast to stage 6 control embryos (left side). Black asterisks denote the location of pole cells initiating dorsal movements at mid-stage 6 (at 10 min after initiation of mesoderm invagination into the wild type).

Fig. 5. Fog-dependent mechanical induction of collective MyoII apical redistribution and apical constriction by Snail-dependent stochastic constrictions. (A) In silico simulations from reference [21] implemented with a mix of Snail-dependent stochastic contraction of cells and Fog-dependent apex constriction of mesodermal cells in response to stress, with Fog ectopically expressed homogenously (Fog+), compared to simulation of the wild type (WT). Lines show hydrodynamics velocity field. Colors encode for the value of velocities: Red and blue are strong; yellow and light blue are weak. (**B)** A schematic showing that the second collective constriction wave depends on both input from Twist and from a mechanical signal that arises from the Snail-induced stochastic constriction wave.

Supplementary Materials

Fig. S1. Morphological phenotypes of *sna* homozygous mutants.

Fig. S2. A minority of *sna-/sna-* embryos exhibit ventral flattening and limited MyoII apical concentration.

Fig. S3. *sna* mutants do not rescue in response to simple contact.

Fig. S4. *twi* mutants that are defective in *sna* expression that express *Fog* in the mesoderm lack Twist.

Fig. S5: Mechanical deformation fails to rescue *twi* mutants that are also defective in *sna* expression.

Fig. S6. Fog and MyoII localization is not altered by heat shock in *sna* mutant embryos.

Fig. S7: sna- and sna- fog + phenotypes predicted by simulations.

REFERENCES

1. Lawrence, P.A. *The making of a fly. The genetics of animal design*. (Oxford; 1992).
2. St Johnston, D. & Nusslein-Volhard, C. The origin of pattern and polarity in the Drosophila embryo. *Cell* **68**, 201-219. (1992).

3. Keller, R., Davidson, L.A. & Shook, D.R. How we are shaped: The biomechanics of gastrulation. *Differentiation* **71**, 171-205 (2003).
4. Tokoyama, Y., X.G., P., Wells, A.R., Kierart, D.P. & Edwards, G.S. Apoptotic force and tissue dynamics during drosophila embryogenesis. *Science* **321**, 1683-1686 (2008).
5. Dawes-Hoang, R.E. *et al.* folded gastrulation, cell shape change and the control of myosin localization. *Development* **132**, 4165-4178 (2005).
6. Bertet, C., Sulak, L. & Lecuit, T. Myosin-dependent junction remodelling controls planar cell intercalation and axis elongation. *Nature* **429**, 667-671 (2004).
7. Blankenship, J.T., Backovic, S.T., Sanny, J.S., Weitz, O. & Zallen, J.A. Multicellular rosette formation links planar cell polarity to tissue morphogenesis. *Dev Cell* **11**, 459-470 (2006).
8. Desprat, N., Supatto, W., Pouille, P.A., Beaurepaire, E. & Farge, E. Forces Driven by Morphogenesis Modulate Twist Expression to Determine Anterior-Midgut Differentiation in Drosophila Embryos. *Dev Cell* **15**, 470-477 (2008).
9. Somogyi, K. & Rorth, P. Evidence for tension-based regulation of Drosophila MAL and SRF during invasive cell migration. *Dev Cell* **7**, 85-93 (2004).
10. Farge, E. Mechanical induction of twist in the Drosophila foregut/stomodeal primordium. *Curr Biol* **13**, 1365-1377 (2003).
11. Wozniak, M. & Chen, C.S. Mechano-tranduction: a growing role for contractibility. *Nat Rev Mol Cell Bio* **10**, 34-43 (2009).
12. Sweeton, D., Parks, S., Costa, M. & Wieschaus, E. Gastrulation in Drosophila: the formation of the ventral furrow and posterior midgut invaginations. *Development* **112**, 775-789. (1991).
13. Kam, Z., Minden, J.S., Agard, D.A., Sedat, J.W. & Leptin, M. Drosophila gastrulation: analysis of cell shape changes in living embryos by three-dimensional fluorescence microscopy. *Development* **112**, 365-370 (1991).
14. Costa, M., Wilson, E.T. & Wieschaus, E. A putative cell signal encoded by the folded gastrulation gene coordinates cell shape changes during Drosophila gastrulation. *Cell* **76**, 1075-1089 (1994).
15. Ip, Y.T., Maggert, K. & Levine, M. Uncoupling gastrulation and mesoderm differentiation in the Drosophila embryo. *Embo J* **13**, 5826-5834 (1994).
16. Costa, M., Sweeton, D. & Wieschaus, E. Gastrulation in Drosophila: cellular mechanisms of morphogenetic movements., in *"The development of Drosophila Melanogaster"*. (eds. M. Bate & A. Martinez-Arias) 425-464 (Cold Spring Harbor Laboratory Press, 1993).
17. Martin, A.C., Kaschube, M. & Wieschaus, E.F. Pulsed contractions of an actin-myosin network drive apical constriction. *Nature* (2008).
18. Morize, P., Christiansen, A.E., Costa, M., Parks, S. & Wieschaus, E. Hyperactivation of the folded gastrulation pathway induces specific cell shape changes. *Development* **125**, 589-597 (1998).
19. Seher, T.C., Narasimha, M., Vogelsang, E. & Leptin, M. Analysis and reconstitution of the genetic cascade controlling early mesoderm morphogenesis in the Drosophila embryo. *Mech Dev* **124**, 167-179 (2007).
20. Leptin, M. twist and snail as positive and negative regulators during Drosophila mesoderm development. *Genes Dev* **5**, 1568-1576 (1991).
21. Pouille, P.A. & Farge, E. Hydrodynamic simulation of multicellular embryo invagination. *Phys Biol* **5**, 15005 (2008).

22. Rauch, C., Brunet, A.C., Deleule, J. & Farge, E. C2C12 myoblast/osteoblast transdifferentiation steps enhanced by epigenetic inhibition of BMP2 endocytosis. *Am J Physiol Cell Physiol* **283**, C235-243. (2002).
23. Raucher, D. & Sheetz, M.P. Membrane expansion increases endocytosis rate during mitosis. *J Cell Biol* **144**, 497-506 (1999).
24. Groulx, N., Boudreault, F., Orlov, S.N. & Grygorczyk, R. Membrane reserves and hypotonic cell swelling. *J Membr Biol* **214**, 43-56 (2006).
25. Odell, G.M., Oster, G., Alberch, P. & Burnside, B. The mechanical basis of morphogenesis. I. Epithelial folding and invagination. *Dev Biol* **85**, 446-462 (1981).
26. Hove, J.R. *et al.* Intracardiac fluid forces are an essential epigenetic factor for embryonic cardiogenesis. *Nature* **421**, 172-177 (2003).
27. Le Beyec, J. *et al.* Cell shape regulates global histone acetylation in human mammary epithelial cells. *Exp Cell Res* **313**, 3066-3075 (2007).
28. Dedman, A. *et al.* The mechano-gated K(2P) channel TREK-1. *Eur Biophys J* (2008).
29. Sawada, Y. *et al.* Force sensing by mechanical extension of the Src family kinase substrate p130Cas. *Cell* **127**, 1015-1026 (2006).
30. Kolsch, V., Seher, T., Fernandez-Ballester, G.J., Serrano, L. & Leptin, M. Control of Drosophila gastrulation by apical localization of adherens junctions and RhoGEF2. *Science* **315**, 384-386 (2007).
31. Hamant, O. *et al.* Developmental patterning by mechanical signals in Arabidopsis. *Science* **322**, 1650-1655 (2008).
32. Terenna, C.R. *et al.* Physical mechanisms redirecting cell polarity and cell shape in fission yeast. *Curr Biol* **18**, 1748-1753 (2008).
33. Wolpert, L. *et al. Principles of Development*. (Oxford University Press, 2002).
34. Jaegerstem, G. The early phylogeny of the metazoa. The bilaterogastrea theory. *Zoot.Bidrag.(Uppsala)* **30**, 321-354 (1956).
35. Wolpert, L. Gastrulation and the evolution of development. *Dev Suppl*, 7-13. (1992).
36. Royou, A., Field, C., Sisson, J.C., Sullivan, W. & Karess, R. Reassessing the role and dynamics of nonmuscle myosin II during furrow formation in early Drosophila embryos. *Mol Biol Cell* **15**, 838-850 (2004).
37. Roth, S. Mechanisms of dorsal-ventral axis determination in Drosophila embryos revealed by cytoplasmic transplantations. *Development* **117**, 1385--1396 (1993).
38. Lehmann, R. & Tautz, D. In situ hybridation to RNA, in *Drososphila Melanogaster: practical uses in cell and molecular biology.* (eds. L.S.B. Glodstein & E.A. Fyrberg) 575-598 (Academic Press, San Diego; 1994).
39. Muller, H.A. & Wieschaus, E. armadillo, bazooka, and stardust are critical for early stages in formation of the zonula adherens and maintenance of the polarized blastoderm epithelium in Drosophila. *J Cell Biol* **134**, 149-163 (1996).

Acknowledgements: This work was funded by the HSFP (RGP0014/2006) and ANR (06PCVI001302) and by a Microsoft PhD fellow grant to PAP. We thank Joanne Whitehead for her suggestions and reading of the manuscript. PAP realized the simulations, mechanical cuts and imaging, PA the indent experiments and imaging, ACB the ShiSna experiments, PAP and EF designed the experiments with PA, and EF coordinated the work.

A

sna-/sna- Stage6

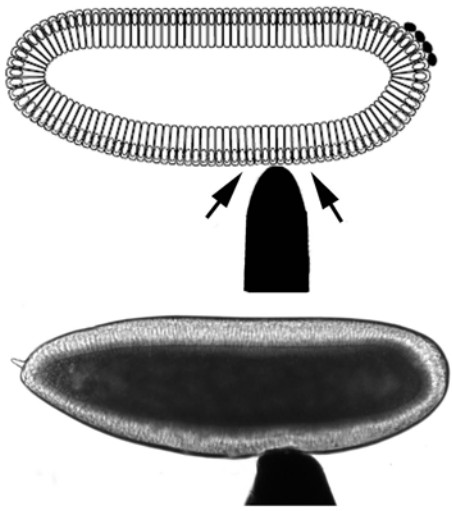

B

sna-/sna- non indented

sna-/sna- indented

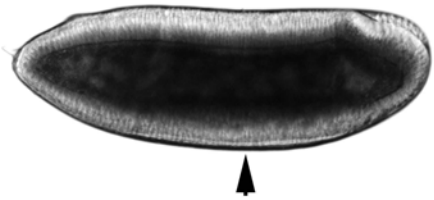

C

Penetrance of apical MyoII redistribution (M) and mesoderm invagination (I)

Embryo Type	Control	Perturbed
Wild Type	Apical Myosin: 100% with invagination	NA
sna-/sna-	M= 25% (partial), with ventral flattening only	**Indented** M=93% I=67% (indented 2-3 min after cellularization). M=100% I=38% (indented 10min after the end of cellularization). **Global deformation** M=64% I=64% with unclosed invagination (deformed at stage6) **Touched** M=0% I=0% **Heat shocked (30°C)** M= 0% I=0%
twi-sna-/twi-sna-	M= 0% I=0%	**Indented** M= 0% I=0%
twi-sna-/twi-	M=0% I=0%	**Indented** M=0% I=0%
twi-sna-/twi-;PE-Fog	M=0% I=0%	**Indented** M=100% I=100%
sna- shi-/sna-shi-	**Endocytosis permissive temperature (20°C)** M=0% I=0%	**Endocytosis blocked temperature (30°C)** M=100% I=100%

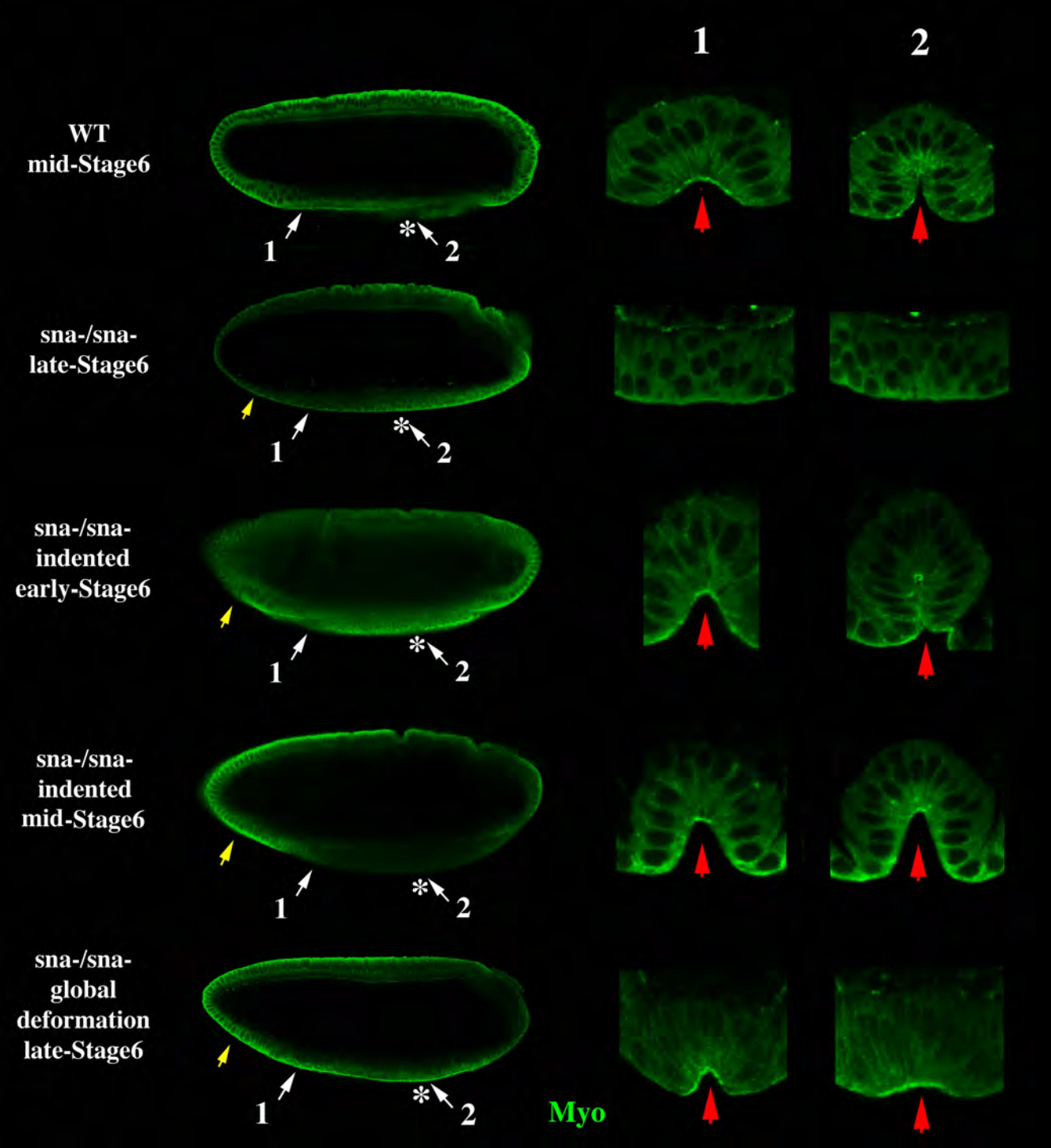
1
2
WT
mid-Stage6
1
2
sna-/sna-
late-Stage6
1
2
sna-/sna-
indented
early-Stage6
1
2
sna-/sna-
indented
mid-Stage6
1
2
sna-/sna-
global
deformation
late-Stage6
1
2
Myo

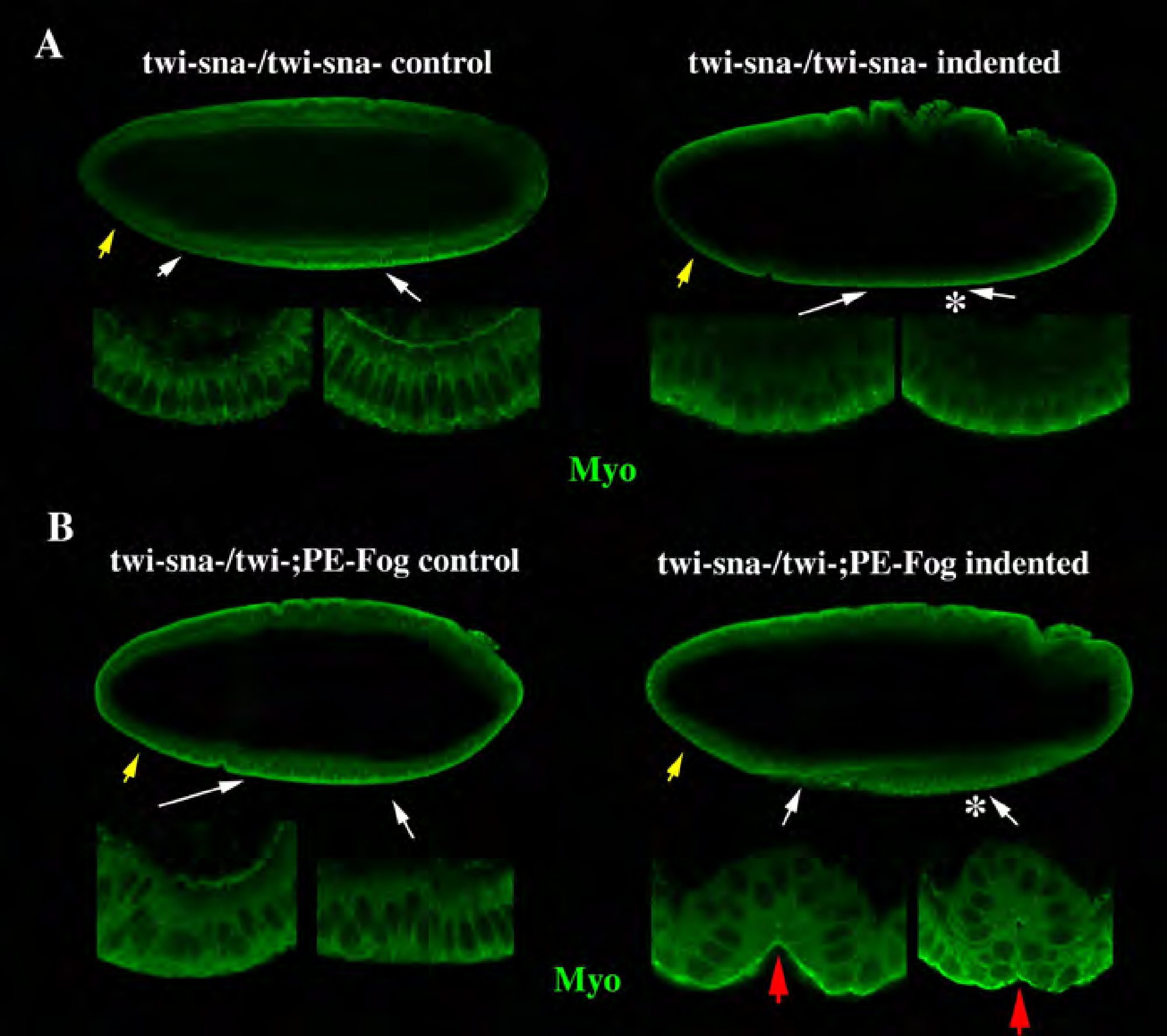
A
twi-sna-/twi-sna- control
twi-sna-/twi-sna- indented
Myo
B
twi-sna-/twi-;PE-Fog control
twi-sna-/twi-;PE-Fog indented
Myo

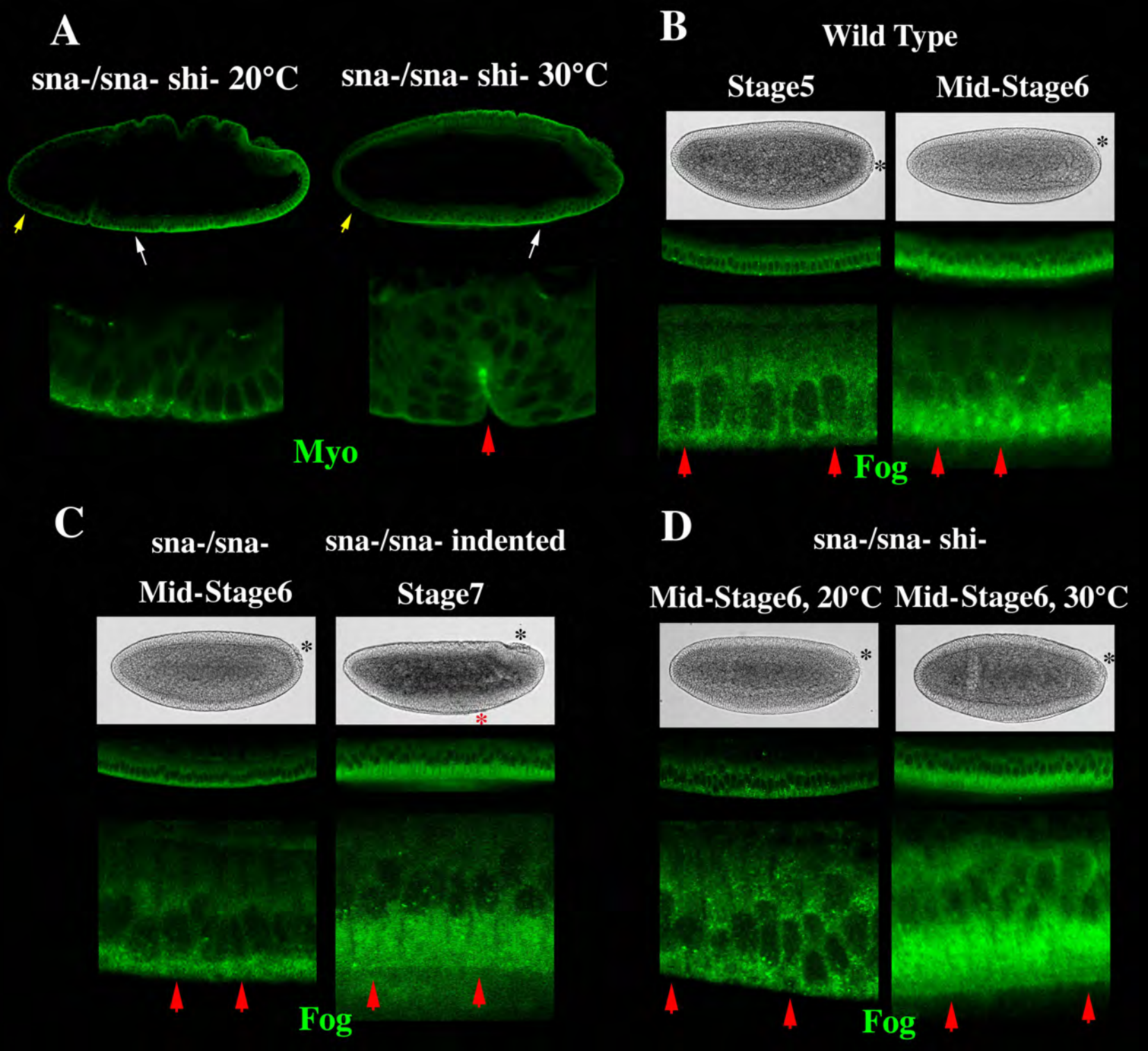
A
sna-/sna- shi- 20°C
sna-/sna- shi- 30°C
Myo
B
Wild Type
Stage5
Mid-Stage6
Fog
C
sna-/sna-
Mid-Stage6
sna-/sna- indented
Stage7
Fog
D
sna-/sna- shi-
Mid-Stage6, 20°C
Mid-Stage6, 30°C
Fog

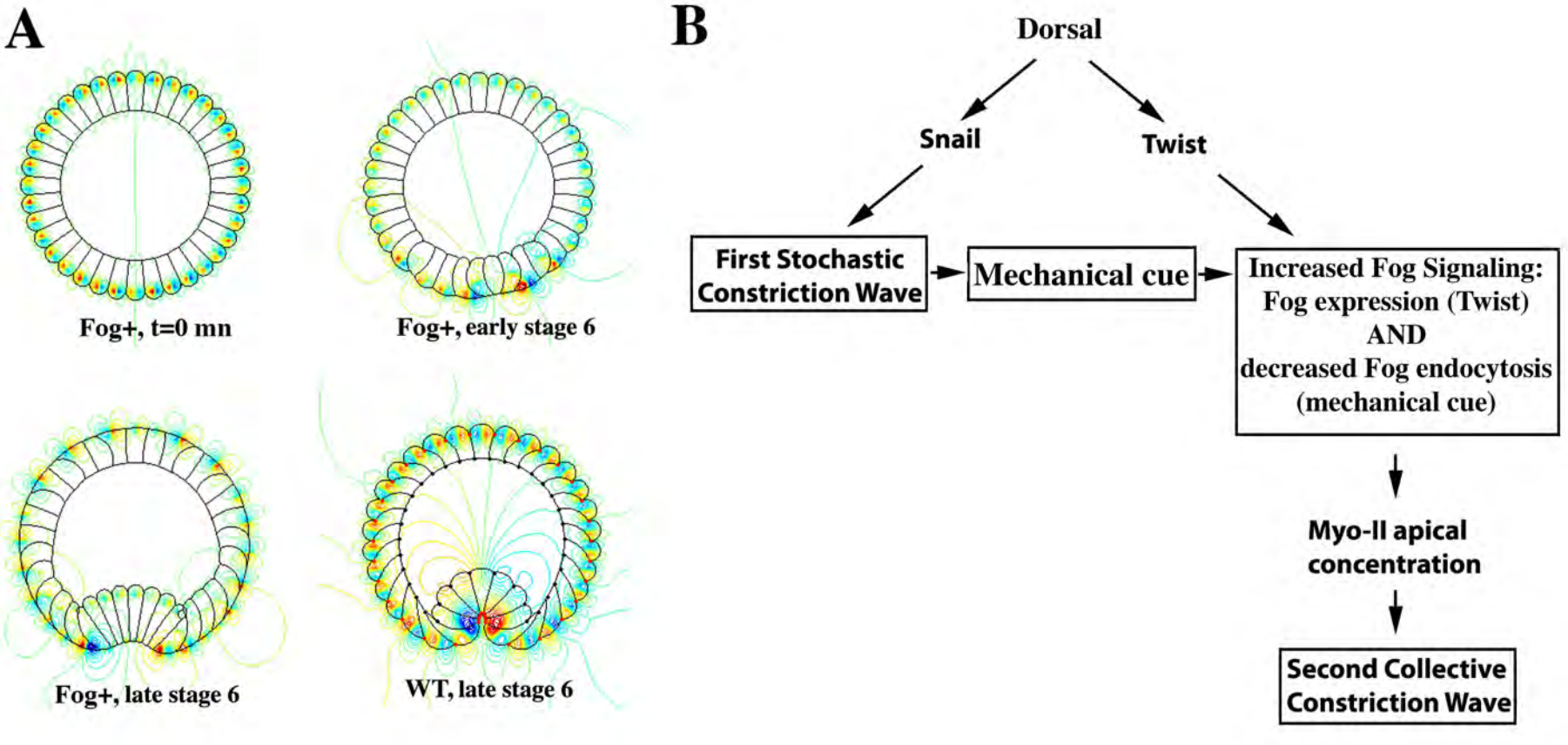
A
Fog+, t=0 mn
Fog+, early stage 6
Fog+, late stage 6
WT, late stage 6
B
Dorsal
Snail
Twist
First Stochastic Constriction Wave
Mechanical cue
Increased Fog Signaling: Fog expression (Twist) AND decreased Fog endocytosis (mechanical cue)
Myo-II apical concentration
Second Collective Constriction Wave

Supplementary Materials

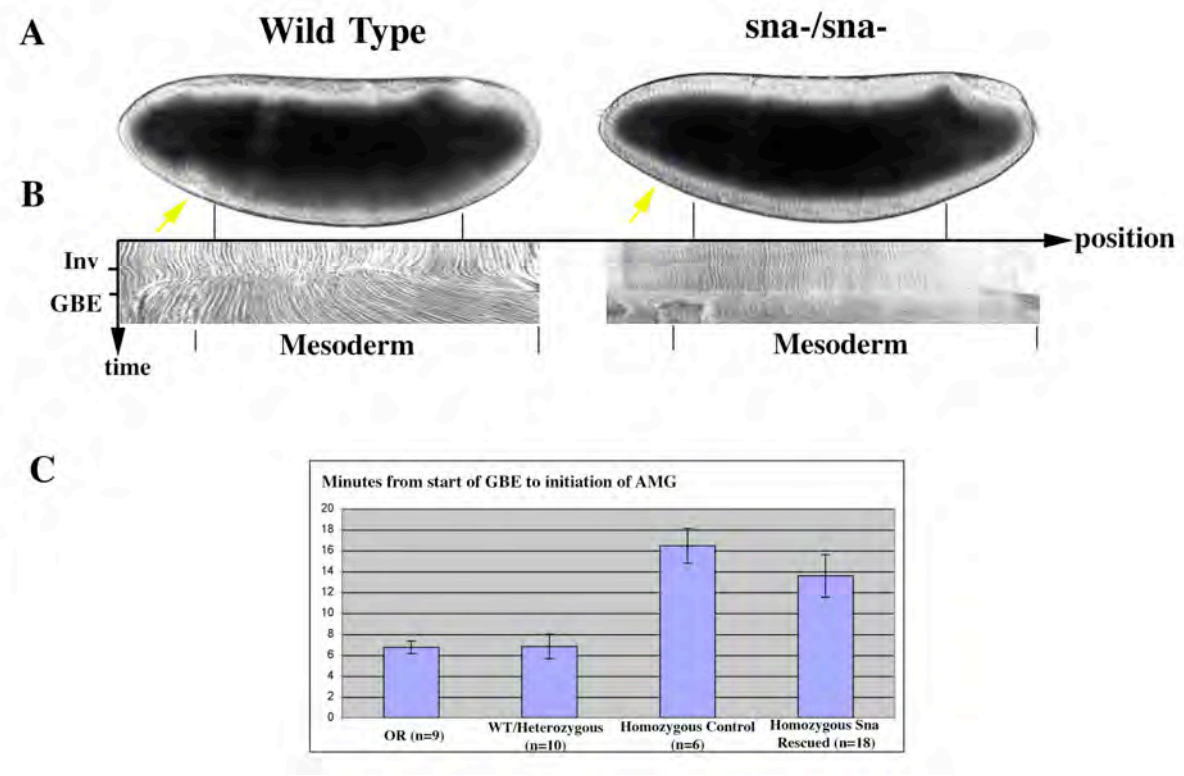

Fig. S1: Morphological phenotypes of *sna* homozygous mutants. (A) Late stage 6 embryos during the first 10 minutes of germ-band extension (GBE), with wild-type embryos, but not *sna-/sna-* embryos, showing the initiation of the anterior midgut (AMG) (yellow arrows). **(B)** Kymograph of the mesoderm sagittal view showing the compression associated with the apex contraction that leads to mesoderm invagination in the wild type. This precedes the dilation that signals GBE. No compression phase is seen in the non-invaginating embryos, characterising *sna-/sna-* mutant. The small black transversal black bars delimit the mesoderm. **(C)** Initiation of AMG formation in wild type, homozygous, heterozygous, and homozygous-rescued embryos. Time zero is the initiation of GBE. Homozygous *sna-* rescued embryos are those in which mechanical indentation was applied. Error bars show standard deviation.

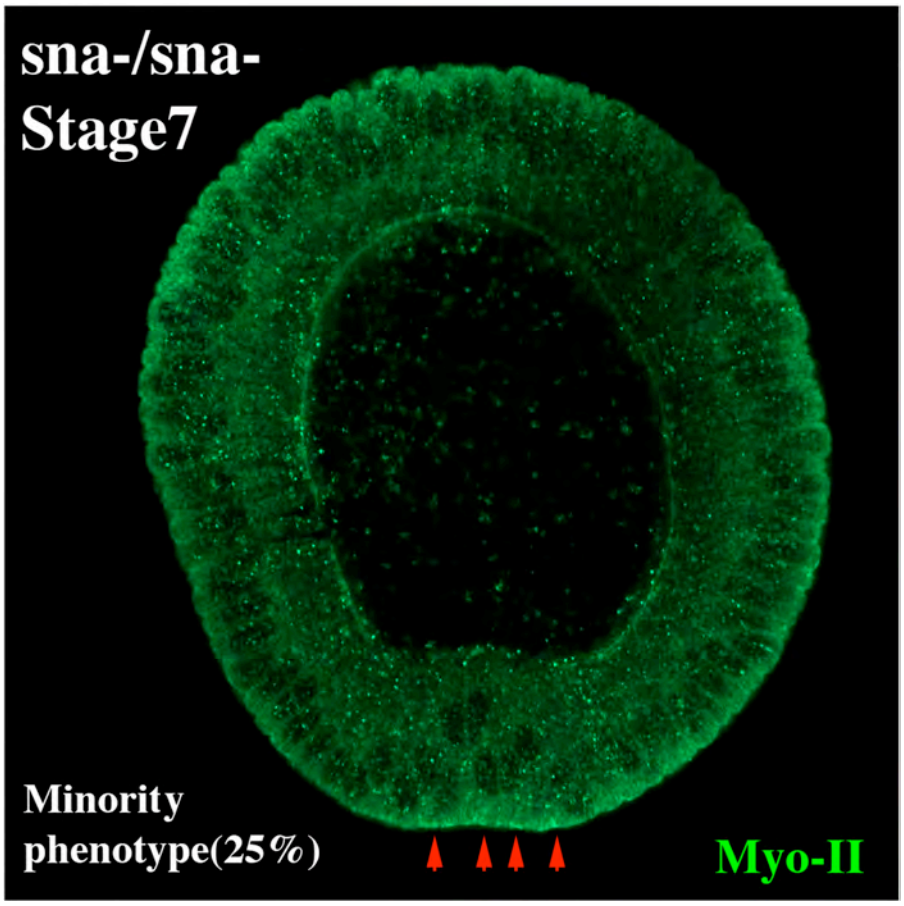

Figure S2: A minority of *sna-/sna-* embryos exhibit ventral flattening and limited MyoII apical concentration. In 25% of cases (n=8), a slight redistribution of Myo-II to the apical side of the cells was observed and was associated with a small inward curvature (red arrowheads) observed in stage 7 *sna* homozygous mutant embryos.

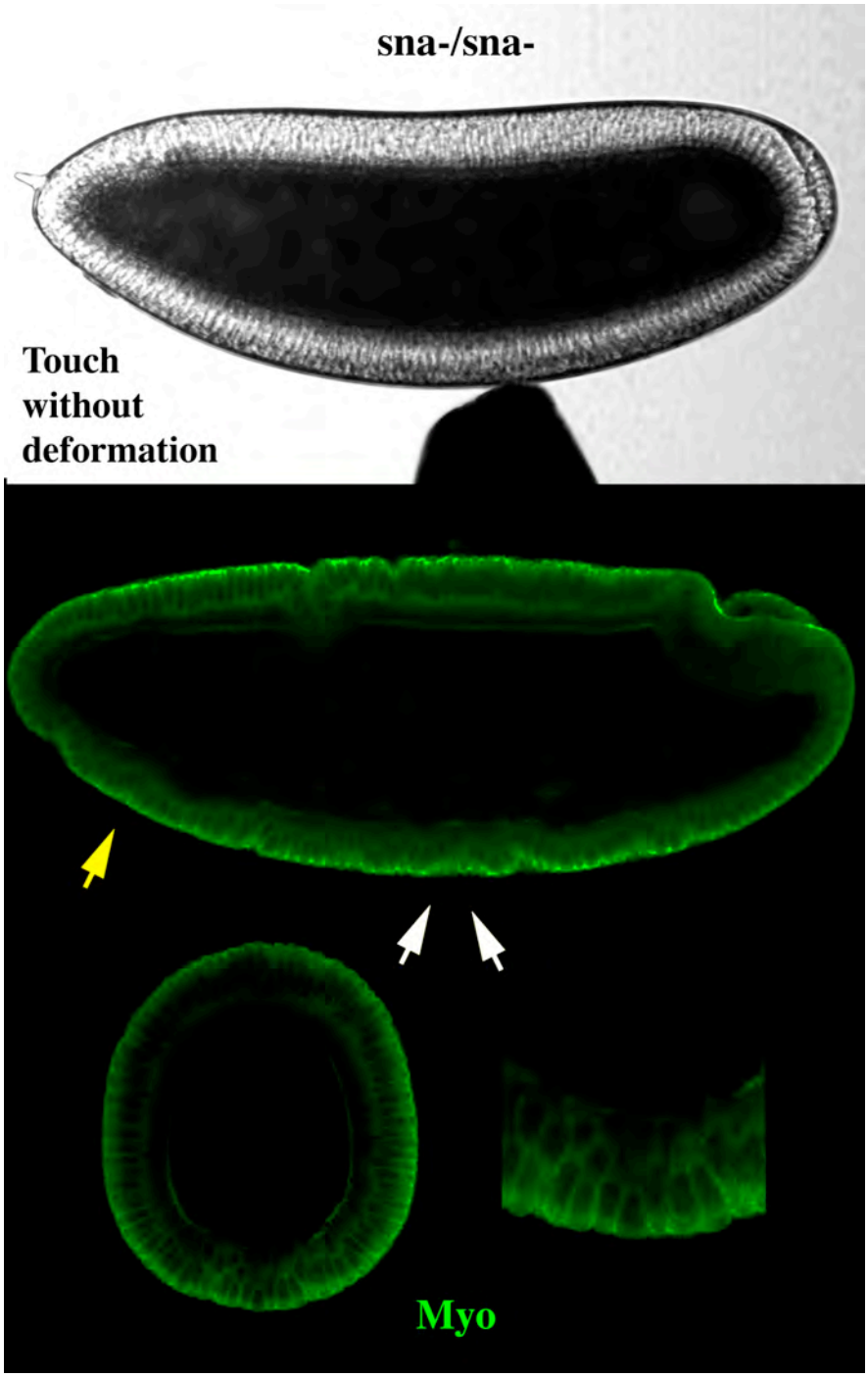

Fig. S3: *sna* mutants do not rescue in response to simple contact. Contact without deformation fails to rescue MyoII apical redistribution and mesoderm invagination in *sna* mutant embryos. Anterior invagination delay (yellow arrows) and lack of mesoderm sagittal compression at stage 6 are phenotypes used to select *sna* homozygotes (see Experimental Procedures section, Fig. S1).

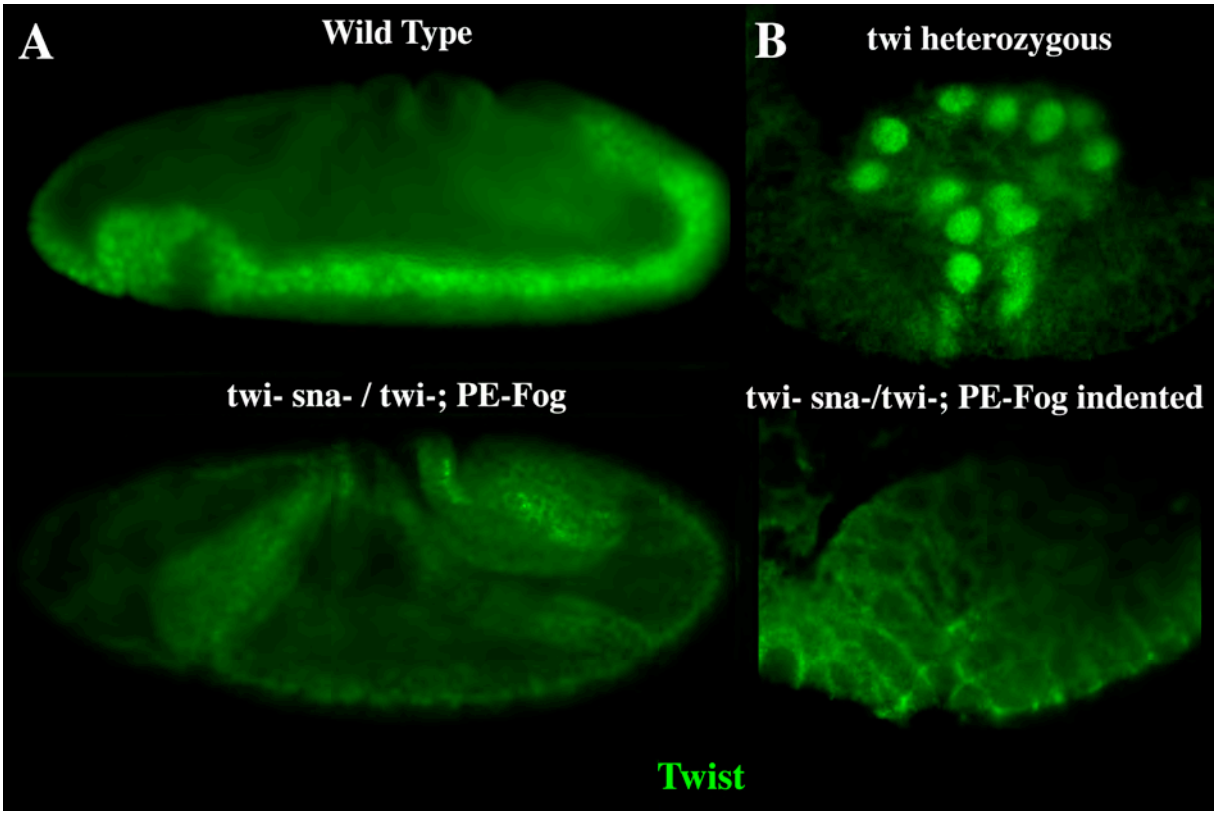

Fig. S4: *twi* mutants that are defective in *sna* expression that express *Fog* in the mesoderm lack Twist. (A) Twist is abundant in the mesoderm in early stage 8 wild-type embryos, but is lacking from the mesoderm in *twi sna / twi; PE-Fog* embryos. (**B**) Expression of Twist is lacking in *twi-sna-/twi-PE-Fog* indented having invaginated at stage 8 (down), to be compared to invaginating heterozygous *twi-sna-/+ and +/twi-PE-Fog* embryos showing an invagination (up). Twist was detected with an a-Twi anti-body and fluorescence images in (A) and confocal in (B) were obtained.

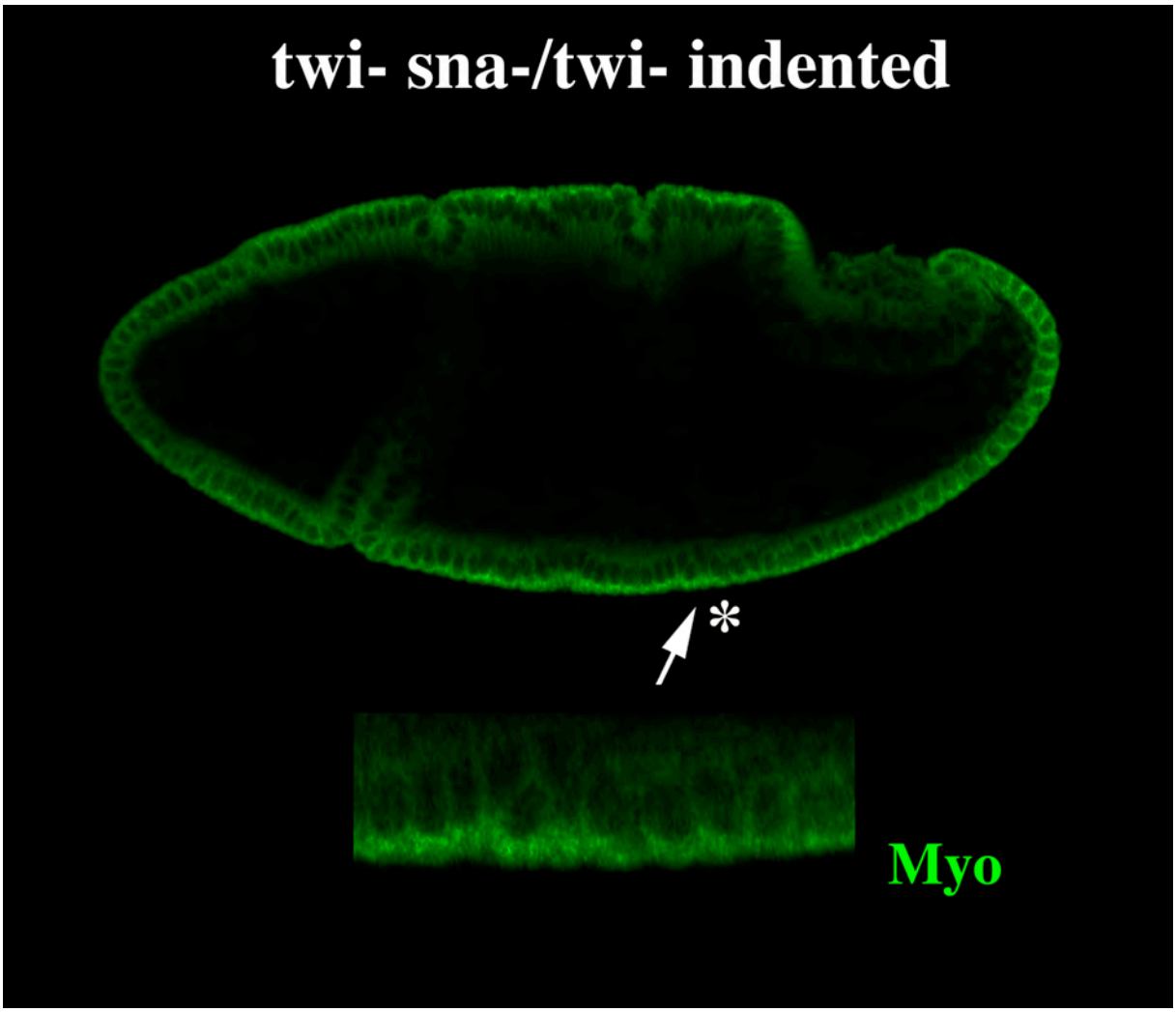

Fig. S5: Mechanical deformation fails to rescue *twi* mutants that are also defective in *sna* expression. Local indentation does not restore mesoderm invagination or apical MyoII redistribution in *twi sna /twi* embryos. MyoII remains punctual and cytoplasmic all around the embryo, which is characteristic of stage 7 non-mesodermal cells.

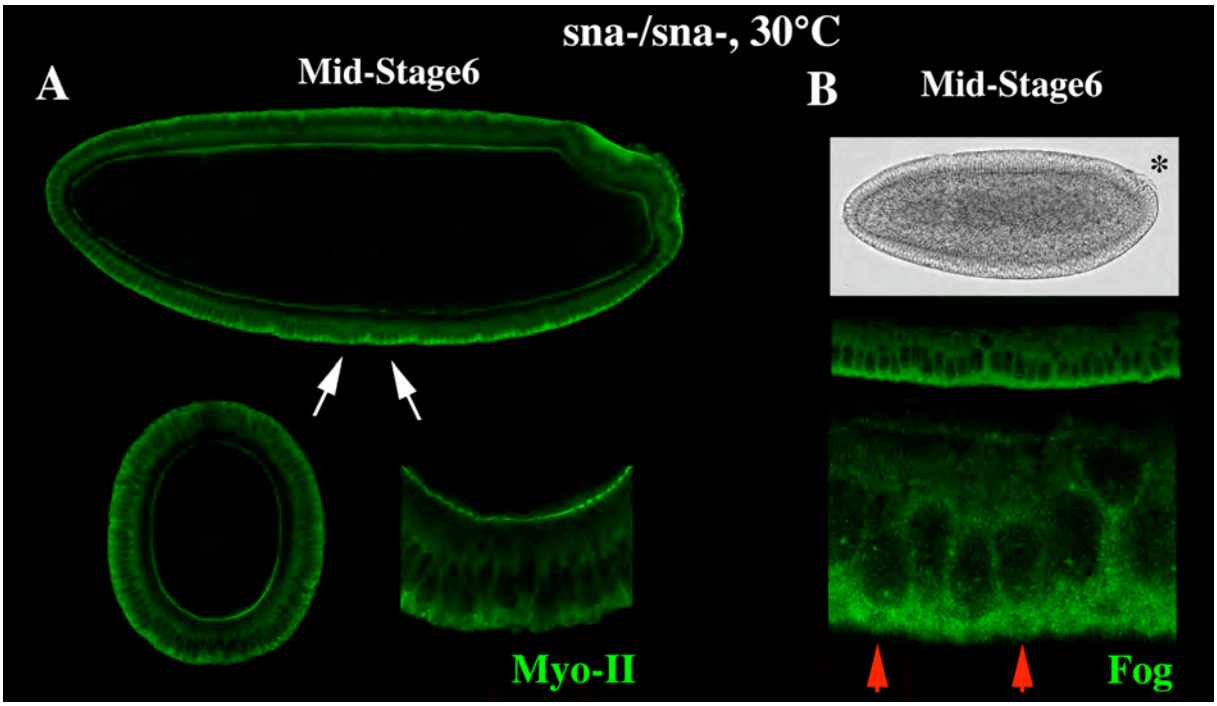

Fig. S6: Fog and MyoII localization is not altered by heat shock in *sna* mutant embryos. **(A)** *sna* embryos do not show MyoII apical redistribution in response to heat shock at 30°C. (**B)** Fog fails to accumulate at the cell surface (red arrows), following heat shock at 30°C, and mesodermal cells show limited apical redistribution of Fog in response to heat shock at 30°C. Black stars denote the location of pole cells initiating dorsal movements at mid-stage 6 (10 min after initiation of mesoderm invagination in the wild type).

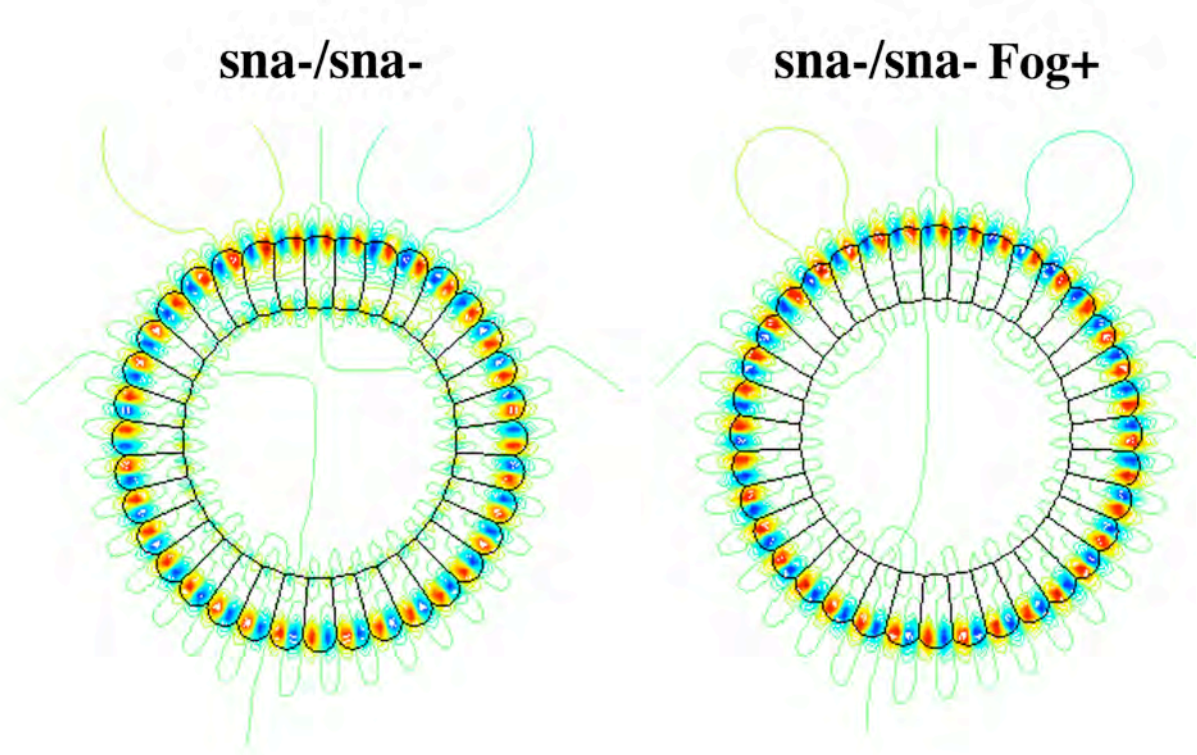

Figure S7: sna- and sna- fog + phenotypes predicted by simulations.

Sna-/sna-: the weak activity of Fog due to the balance between expression and degradation of Fog leads to partial slight flattening of mesoderm apices, possibly reflecting the 25% of the *sna* embryos found with ventral flattening (Fig. S2). **Sna-/sna- fog+:** expression of Fog all around the *sna* embryo in addition to the endogenous Twist induced mesoderm expression leads to partial apical flattening of all cells, due to Fog weak activity. Apical flattening all around the embryo is observed within these experimental conditions in *sna hs-fog* embryos (in which expression of Fog could be over-expressed compared to endogenous expression, leading to stronger flattening effects than in the simulation) [1].

The equations of the simulation follow the stationary incompressible fluid dynamics at low Reynolds number governed by the two equations:

Div V = 0 (1.a)

ν . **Δ V** = **Grad** P (1.b),

where P is the pressure, V the velocity and $\nu=\eta/\rho$, the ratio between the viscosity and the density of the fluid.

The function Ψ, solution to equations (1), was used to simulate the movements of membrane domes into the fluid:

$\Psi = 4 \, . \, l \, /2 \, . \, V_\Psi \, . \, \psi(\rho=2 \, r \, / \, l \, , \, \phi)$ (2),

with $\psi(\varrho, \phi) = \varrho \, / \, (\, 1 + \varrho \,)^{2}.\sin \phi$. *l* is the distance between the two extremities of the dome, V_Ψ is the mean value of the fluid velocity in between the two extremities of the dome, and (r, ϕ) are cylindric coordinates [2].

References

1. Morize, P., Christiansen, A.E., Costa, M., Parks, S. & Wieschaus, E. Hyperactivation of the folded gastrulation pathway induces specific cell shape changes. *Development* **125**, 589-597 (1998).
2. Pouille, P.A. & Farge, E. Hydrodynamic simulation of multicellular embryo invagination. *Phys Biol* **5**, 15005 (2008).